Interacting scalar fields: Dark matter and early dark energy

Gabriela Garcia-Arroyo,[1,*] L. Arturo Ureña-López,[2,†] and J. Alberto Vázquez[1,‡]
[1]Instituto de Ciencias Físicas, Universidad Nacional Autónoma de México, 62210, Cuernavaca, Morelos, México
[2]Departamento de Física, DCI, Campus León, Universidad de Guanajuato, 37150, León, Guanajuato, México

(Received 16 February 2024; accepted 18 June 2024; published 22 July 2024)

The main aim of this work is to explore the possibility that cold dark matter (CDM) and early dark energy (EDE) can be described by canonical scalar fields that are coupled at the level of its conservation equations. The formalism covers dynamical aspects at the background and linear perturbation levels for an arbitrary coupling function, followed by an example of it. We emphasize the impact of this model on the matter power spectrum and the cosmic microwave background (CMB) spectra, with or without direct interaction. Our findings indicate that the presence of a scalar field can partially counteract the known effects of the other, opening the possibility to avoid some undesired aspects, such as the increase in Ω_m that usually is needed in the case of a purely EDE scalar field scenario, in order to fit the CMB spectra. This opens up the possibility to analyzing whether the interaction can help to ameliorate the cosmological tensions.

DOI: 10.1103/PhysRevD.110.023529

I. INTRODUCTION

One of the main conundrums of modern cosmology is the explanation of the dynamics of the Universe, led by two still-unknown components called dark energy and dark matter. These ingredients are the foundations of the standard cosmological model, or ΛCDM. Here, the cosmological constant (Λ) plays the key role of dark energy and it is considered to be responsible for the current accelerating expansion of the Universe, suggested by many cosmological observations [1,2]; whereas the cold dark matter (CDM) is the principal component for structure formation which significantly contributes to the observed rotation curves of galaxies [3]. Despite the simplicity of the model and that it provides a very accurate description to the majority of the astronomical observations, it carries out several issues of fundamental nature, i.e., at the largest scales the cosmological constant problems [4,5] or the recent H_0 tension [6]; at the galactic levels, the unexplained central density behaviors in halos and the overpopulation of small substructures [7,8]. Therefore, a viable alternative to replace the standard description of such components is the scalar fields, to behave as dark matter [9–12], dark energy [13–16], or inflation [17–20]. However, to achieve these characteristics, it is still necessary to specify the potential of the field and its initial conditions.

The idea of replacing cold dark matter for scalar fields was considered a couple of decades ago, with the simplest possibility of a real field, minimally coupled to gravity, and interacting only gravitationally with ordinary matter [21–23]. The requirement for the scalar field, ϕ, to mimic a pressureless fluid is to include a convex potential with a minimum at some value of the field, ϕ_c, such that the mass of the associated particle could be non-null. An example of such a type is the parabolic function $V(\phi) = 1/2 m_\phi^2 \phi^2$ whose mass is defined as standard, $m_\phi^2 = \partial_\phi^2 V(\phi_c)$ [24,25]. However, depending on the particular form of the potential, it may experience different behaviors before acting like a pressureless fluid, hence several alternatives are also brought into consideration, i.e., the self-interacting potential with a quartic term contribution $V(\phi) = 1/2 m_\phi^2 \phi^2 + \lambda_\phi \phi^4$ [26–29], the axionlike or trigonometric potential $V(\phi) = m_\phi^2 f^2 [1 + \cos(\phi/f)]$ [30,31] and its analog $V(\phi) = m_\phi^2 f^2 [\cosh(\phi/f) - 1]$ [32,33]. The dynamics of these and some other potentials has been studied extensively in detail [34], as well as the combination of two scalar fields with different contributions to the total DM [35].

With a similar idea in mind, scalar fields may also play an important role leading to dynamical dark energy models. Here, the task is to be able to imitate the cosmological constant behavior at late times, by including a minimally couple to gravity field with a kinetic energy term, which its positive sign corresponds to quintessence and the negative to phantom; and also a given potential. The quintessence model is considered as the simplest scenario with no

*Contact author: arroyo@icf.unam.mx
†Contact author: lurena@ugto.mx
‡Contact author: javazquez@icf.unam.mx

theoretical problems, such as the appearance of ghosts or Laplacian instabilities, that describes a dark energy evolving over time [36,37]. These types of models are often classified into two broad categories such as "thawing" or "freezing" [38,39] depending on their behavior over time. A step further is to test a collection of potentials and compare its statistical viability in terms of current observations [40–43], or to include more than a single scalar field [44–48] to be able to reproduce the crossing of the phantom-divide line (PDL) shown by several model-independent reconstructions [49–52].

Moreover, there is another type of scalar field potentials, named early dark energy (EDE) [53,54], that could have a non-negligible contribution during the early universe, prior to the onset of the current dark-energy-dominated epoch, where it is responsible of the accelerated expansion of the universe. If the fraction of this early dark energy is large enough, it could have strongly affected the physics of the early universe and left its signature in the cosmic microwave background radiation and matter power spectrum. There are different EDE potentials, one of the most studied being the axionlike potential, denoted by $V(\phi) = m^2 f^2[1 - \cos(\phi/f)]^n$. This potential has been inspired by ultralight axions (ULA) from string theory [55–57]. It is important to note that ultralight axions are also candidates for dark matter [58,59]. Essentially, a ULA behaves as DE when its mass value is within the range $m_\phi \lesssim 10^{-27}$ eV, whereas in the opposite mass range it dilutes away as DM. In this work, without loss of generality, we focus on the EDE models with an Albrecht-Skordis (AS) potential; in [60,61] the authors discuss some of its properties with emphasis in the cosmological eras and in view of the ability to explain the available observations of that epoch. A more recent work [62] also explores the ability of the model to solve the H_0 tension and the possible connections with different extensions of ΛCDM. The dynamics of the AS potential allows us to have an almost constant EDE contribution during the early universe, modulated by the potential's parameters. In fact, it mimics the behavior of radiation, then it begins to decay at a scale factor around 10^{-6}, reaches a minimum at approximately 10^{-1} before transitioning into a growth phase to attain the characteristics of the late dark energy. Importantly, the AS potential does not require the inclusion of a cosmological constant.

Even though single scalar field models provide a very good description of the evolution of the cosmological densities and peaks of the cosmic microwave background (CMB), as well as the number of substructures in galaxy arrays [24,25,63,64], they still present some open issues, for example, for scalar field dark matter (SFDM) numerical simulations have shown that the mass of the field could vary for different scales of the simulation in order to fit the observations [65]; while for dark energy, a single scalar field is not able to cross the PDL as shown in several results [44]. Hence, the inclusion of more than a single field has come to the rescue. Other areas have come up with similar ideas where two or more fields are used, for instance, a combination of the inflaton and the SFDM [27], the inflaton and the curvaton [66], two scalar fields to account for inflation [67,68], to dark energy [46] or to dark matter [35], interactions between dark energy and dark matter [69].

Until now, neither cosmology nor particle physics has provided a definitive theory to describe the DM or DE. In this work we open up the possibility that both dark matter and dark energy may be composed of scalar fields, with different potentials, and with the addition of a nonminimal interacting term, we called it scalar field interacting early dark energy (SF-IEDE). In this regard, there are different methods to introduce the coupling, one of which makes use of the variational approach, adding an interaction Lagrangian [70,71] that couples dark matter as a fluid and dark energy as quintessence. Perhaps the most commonly used approach is to introduce the coupling term at the level of conservation equations [72–74]. In this case, the coupling term could exist when both dark components are modeled as fluids [75], or a quintessence field coupled to dark matter [76–78], and, in our case, when both are scalar fields. However, it is important to emphasize that at some point of the formalism, most of the authors replace the scalar field dark matter with a perfect fluid [79,80], and most of them only focus on the late dark energy contribution. However, there are also proposals for interacting EDE scenarios [81,82] as well. The novelty of this work is that we maintain both components as scalar fields along with the interacting term. For scalar field DM, we utilize the quadratic and axionlike potentials, the latter referred to as trigonometric along this work, while for scalar field EDE, we use the AS potential; the interacting term is explained further below.

The paper is organized as follows. In Sec. II we give a brief overview of the relevant equations for the interacting formalism, at the background and linear perturbation level, we focus on scalar fields. In Sec. III, we present the minimally coupled interacting case, whereas in Sec. IV we explore the consequences of a nonminimally coupling, and finally in Sec. V the main conclusions of the paper are given.

II. INTERACTING SCALAR FIELDS AT THE BACKGROUND AND LINEAR LEVELS

Throughout this work, we consider the dark sector consisting of two canonical scalar fields: one representing early dark energy (quintessence) and the other representing dark matter (SFDM). Each of these fields is coupled to the other components of the universe only through gravity, meaning that their conservation equations are not modified by the presence of the fields. However, for the dark sector, a coupling term is introduced at the level of its conservation equations [83], which allows the exchange of energy and momentum between the scalar fields, and additionally

guarantees that the total energy-momentum tensor remains conserved.

A. Effective coupling

The equations of motion for the background evolution, considering a flat, homogeneous and isotropic universe, are given by

$$\dot{\rho}_\psi = -3H(\rho_\psi + p_\psi) + Q_\psi, \tag{1a}$$

$$\dot{\rho}_\phi = -3H(\rho_\phi + p_\phi) + Q_\phi. \tag{1b}$$

Here, overdot means derivative with respect to cosmic time, H is the Hubble factor, ρ_ψ (p_ψ) and ρ_ϕ (p_ϕ) are the energy densities (isotropic pressures) of the fields ψ and ϕ, respectively. Furthermore, Q_ψ (Q_ϕ) is the rate of energy transfer to the DE component ψ (the DM component ϕ), and due to energy conservation, we find that $Q_\phi = -Q_\psi$. The form of the decay rates of the fields in the dark sector should be derived from first principles, but in the absence of a fundamental theory we have to resort to phenomenological proposals, and some may be more justified than others, see for instance [84] and references therein.

At the fundamental level, both scalar fields evolve according to their Klein-Gordon (KG) equations at both background and linear orders. These equations follow from the conservation of the energy-momentum tensor of a scalar field, which takes the expression $T^{(\phi_A)}_{\mu\nu} = \partial_\mu\phi_A\partial_\nu\phi_A - g_{\mu\nu}[\frac{1}{2}\partial^\alpha\phi_A\partial_\alpha\phi_A + V(\phi_A)]$. In correspondence with the equations of motion (1), at the background level, we find

$$\ddot{\psi} + 3H\dot{\psi} + \partial_\psi V(\psi) = -\frac{Q}{\dot{\psi}}, \tag{2a}$$

$$\ddot{\phi} + 3H\dot{\phi} + \partial_\phi V(\phi) = \frac{Q}{\dot{\phi}}. \tag{2b}$$

Here, $Q = -Q_\psi = Q_\phi$ is an arbitrary function. Note that the sign of the interaction determines the transfer of energy from one component to the other, and for our choice the energy flux goes from the field ψ to the field ϕ. If there is no interaction, $Q = 0$, and then each scalar field evolves independently.

B. Equations of motion

The strategy for solving the coupled KG Eqs. (2) at zeroth order is as follows: given the rapid oscillations regime in the evolution of SFDM, we convert its associated KG equation into a system of first-order differential equations by introducing the following change of variables [31,85]:

$$\Omega_\phi^{1/2}\sin\left(\frac{\theta}{2}\right) = \frac{\kappa\dot{\phi}}{\sqrt{6}H}, \quad \Omega_\phi^{1/2}\cos\left(\frac{\theta}{2}\right) = \frac{\kappa V^{1/2}}{\sqrt{3}H},$$
$$y_1 = -\frac{2}{H}\sqrt{2}\partial_\phi V^{1/2}, \quad y_2 = -\frac{4\sqrt{3}}{H\kappa}\partial_\phi^2 V^{1/2}, \tag{3}$$

where, $\kappa^2 \equiv 8\pi G$, with G the gravitational coupling constant, and $\Omega_\phi = \kappa^2\rho_\phi/3H^2$. This change in variables has been shown to accurately track the evolution of the SFDM system. Applying this change of variables, and analogous to the results in [86], the associated system to Eq. (2b) is

$$\dot{\theta} = -3H\sin\theta + Hy_1 - \frac{\kappa^2\cos(\frac{\theta}{2})}{3H^2\Omega_\phi\sin(\frac{\theta}{2})}Q_\phi,$$
$$\dot{y_1} = \frac{3}{2}H(1+w_T)y_1 + \Omega_\phi^{1/2}\sin\left(\frac{\theta}{2}\right)y_2 H,$$
$$\dot{\Omega}_\phi = 3H\Omega_\phi(w_T - w_\phi) - \frac{\kappa^2}{3H^2}Q_\phi, \tag{4}$$

where w_T corresponds to the total equation of state (EoS), and w_ϕ is the EoS associated to the SFDM. However, for the quintessence component and considering its slow evolution, we will preserve the original variables ψ and $\dot{\psi}$.

At linear order, in Fourier space and in synchronous gauge [87], the evolution of each scalar field is dictated by the perturbed KG equation:

$$\delta\ddot{\psi} + 3H\delta\dot{\psi} + [k^2 + \partial_\psi^2 V(\psi)]\delta\psi + \frac{1}{2}\dot{h}\dot{\psi} = -\delta\left(\frac{Q}{\dot{\psi}}\right), \tag{5a}$$

$$\delta\ddot{\phi} + 3H\delta\dot{\phi} + [k^2 + \partial_\phi^2 V(\phi)]\delta\phi + \frac{1}{2}\dot{h}\,\dot{\phi} = \delta\left(\frac{Q}{\dot{\phi}}\right), \tag{5b}$$

where $\delta\psi$ and $\delta\phi$ are the perturbations of the scalar fields, and h is the trace of the metric perturbation.

To solve the equations, we follow the same line of thought as in the background case. Quintessence will be implemented through Eq. (5a) and for SFDM, i.e., Eq. (5b), we will make use of angular variables,

$$\frac{2}{3}\frac{\kappa\delta\dot{\phi}}{H} = -\Omega_\phi^{1/2}e^\alpha\cos(\vartheta/2), \quad \frac{\kappa y_1\delta\phi}{\sqrt{6}} = -\Omega_\phi^{1/2}e^\alpha\sin(\vartheta/2),$$
$$\delta_0 = -e^\alpha\sin[(\theta-\vartheta)/2], \quad \delta_1 = -e^\alpha\cos[(\theta-\vartheta)/2], \tag{6}$$

then the evolution of Eq. (5b) is given in terms of δ_0 and δ_1, as follows:

$$\dot{\delta}_0 = H[-3\sin\theta - \omega(1-\cos\theta)]\delta_1 + H\omega\sin\theta\delta_0$$
$$-\frac{\dot{h}}{2}(1-\cos\theta) - \sqrt{\frac{2}{3}}\frac{\kappa}{\Omega_\phi^{1/2}}\sin\left(\frac{\theta}{2}\right)\delta\left(\frac{Q}{\dot{\phi}}\right)$$
$$+\frac{\kappa^2 Q}{3H\Omega_\phi}\left[\frac{\delta_0}{2} - \cot\left(\frac{\theta}{2}\right)\delta_1\right], \tag{7}$$

$$\dot{\delta}_1 = \left[-2\cos\theta - \omega\sin\theta + \Omega_\phi^{1/2}\sin\left(\frac{\theta}{2}\right)\frac{y_2}{y_1}\right]H\delta_1 - \frac{\dot{h}}{2}\sin\theta + \left[\omega(1+\cos\theta) - \Omega_\phi^{1/2}\cos\left(\frac{\theta}{2}\right)\frac{y_2}{y_1}\right]H\delta_0 - \sqrt{\frac{2}{3}}\frac{\kappa}{\Omega_\phi^{1/2}}\cos\left(\frac{\theta}{2}\right)\delta\left(\frac{Q}{\dot{\phi}}\right) + \frac{\kappa^2 Q}{3H\Omega_\phi}\left[\frac{\delta_1}{2} + \cot\left(\frac{\theta}{2}\right)\delta_0\right]. \quad (8)$$

Here $\omega = k^2/k_J^2$, with the Jeans scale defined as $k_J^2 \equiv 2a^2H^2y_1$.

Up to this point, the formalism remains general, as we have not specified the quintessence or SFDM potential yet, nor have we assumed a specific expression for the interacting term. It is important to note that, to solve the background and linear equations, these specifics should be provided. In fact, for linear equations, it becomes necessary to substitute the function Q and then perturb the terms $Q/\dot{\psi}$ and $Q/\dot{\phi}$ in Eqs. (5). In the subsequent sections, we will provide examples of these functions to solve the system by modifying the Einstein-Boltzmann solver CLASS,[1] to then obtain the cosmological observables.

III. NONINTERACTING CASE

In this section, as an initial step, we begin by summarizing the key individual characteristics of SFDM and EDE potentials, given that it is common to model the dark sector with only one component as a scalar field. Then, we will explore the scenario where both components are described simultaneously by scalar fields, considering as a first attempt that they are coupled solely through gravity, i.e., $Q = \delta Q = 0$.

A. Background

At the background level, the evolution of each scalar field remains unaffected by the gravitational influence of the other. Due to this characteristic, in this subsection both scalar fields are turned on, and the chosen scalar field parameters to sketch each component are such that at the present time become $\Omega_m = 0.32$ and $\Omega_\psi = 1 - \Omega_m$.

1. Quintessence scalar field

Pure exponential quintessence is known to not provide a transition from a matter-dominated epoch described by a scaling solution, where the contribution of the scalar field is not exactly zero, to an accelerated expansion epoch [36]. Therefore, if we want to have an early scalar field contribution, one approach is to modify the exponential potential. An option we opt to take is to consider the Albrecht-Skordis potential, which additionally has the property that cannot be classified as purely thawing or freezing, the mathematical expression used in this work is [61]:

$$V(\psi) = V_p(\psi)e^{-\lambda\psi} = \{(\psi - B)^2 + A\}e^{-\lambda\psi}, \quad (9)$$

where B, A and λ are constants. In order to achieve late-accelerated expansion and a scaling solution at early times, these constants are not totally independent. For instance, $A\lambda^2 < 1$, and B should be determined by other cosmological observables, see Appendix A for more details of this potential.

Note that in recent work [62,88] the AS potential (9) has been rewritten. At the background level, our focus lies on the evolution of the density and EoS parameters, as depicted in Figs. 1 and 2 respectively. From Fig. 1 we can see that, at early times, $\Omega_\psi \sim 0.028$ is non-negligible and that it is scaling with respect to radiation, as expected. In Fig. 2, we show the EoS parameters of the scalar fields, and also the effective one (defined as $w_T = P_{\rm tot}/\rho_{\rm tot}$), from this figure it is clear that for the AS potential, there is no need to include an additional cosmological constant, since the scalar field can eventually reach a value of $w_\psi = -1$ at late times and hence drives the accelerated expansion of the universe.

2. Scalar field dark matter

The formalism of this work is applicable to the following three different SFDM potentials that can be differentiated by a single parameter λ_ϕ [31], related to the decay constant, f, for instance $\lambda_\phi \equiv \mp 3/\kappa^2 f^2$:

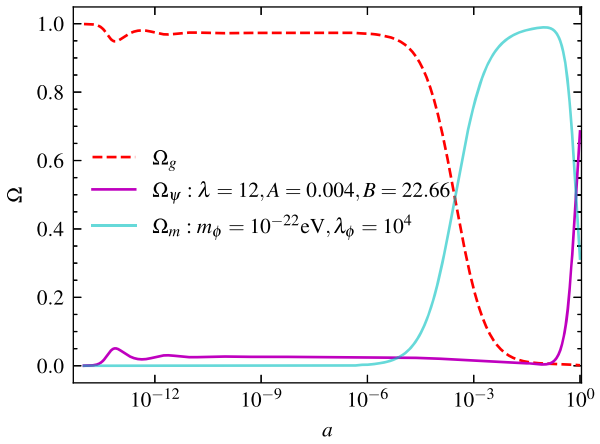

FIG. 1. AS(ψ)-SFDM(ϕ) model. Evolution of the density parameters, including radiation ($\Omega_{\rm g}$), matter ($\Omega_{\rm m}$: SFDM + baryons), and quintessence as dark energy (Ω_ψ). The scalar field parameters are indicated by the labels. This parameter selection allows us to have a moderate, non-null contribution of the quintessence scalar field at early times, while the parameters of the SFDM are chosen for the trigonometric potential.

[1] https://github.com/gabygga/Interacting.git.

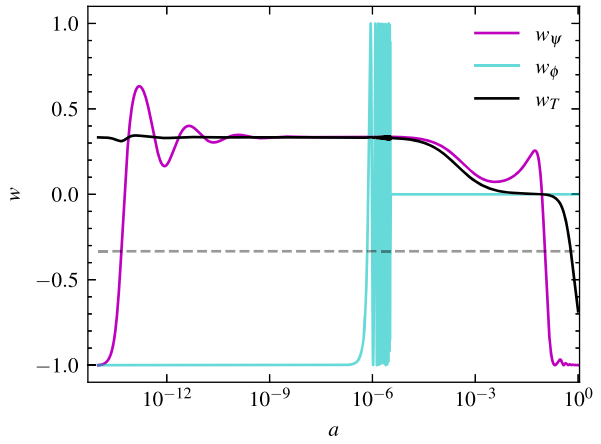

FIG. 2. Evolution of the EoS of the scalar fields with the same parameters as in Fig. 1. The gray dashed line corresponds to $-\frac{1}{3}$.

$$V(\phi) = \begin{cases} m_\phi^2 f^2[1+\cos(\phi/f)], & \lambda_\phi > 0, \\ \frac{1}{2} m_\phi^2 \phi^2, & \lambda_\phi = 0, \\ m_\phi^2 f^2[1+\cosh(\phi/f)], & \lambda_\phi < 0. \end{cases} \quad (10)$$

These potentials drive different background and perturbed density evolution. In Figs. 1 and 2, the evolution of the density and the EoS parameter are plotted for an SFDM mass of 10^{-22} eV and for the trigonometric potential. These plots show that the field evolves similar to CDM but at early times, where its contribution to the total matter content is negligible, there is a period where it evolves similarly to a cosmological constant ($w_\phi \sim -1$) [89].

B. Linear perturbations

1. Quintessence scalar field

As is well known, the scalar field has linear perturbations such that if this field contributes at early times, its perturbations are expected to result in modifications to the CMB and the matter power spectra (MPS). In order to isolate the effects of each field, in this part, we only consider EDE as a scalar field and DM as dust (AS + CDM). To illustrate these modifications, in Fig. 3 we plot the residual CMB-TT spectra and the MPS ratio with respect to ΛCDM, along with three sets of AS parameters to demonstrate their impact. The other baseline ΛCDM parameters are from Planck18 [90] and are the same for all datasets, with the following values: $\omega_b = 0.022$, $\Omega_\phi = 0.264$, $\tau = 0.054$, $A_s = 2.1 \times 10^{-9}$, $n_s = 0.966$, and $h = 0.67$.

Some general aspects are common to these spectra. A lower value of λ corresponds to a larger fraction of EDE during the radiation-dominated epoch, leading to significant suppression of matter perturbations during that period. This implies that smaller λ values result in greater deviations from the reference model. In turn, this suppression of power in the MPS occurs on small scales (large k's), while at smaller k modes, the MPS associated with the AS model

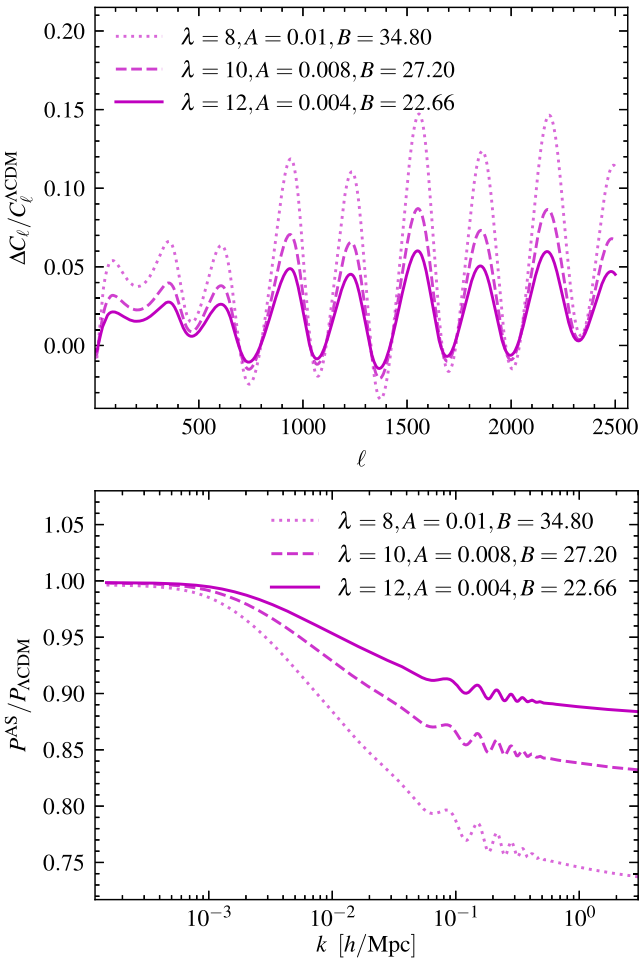

FIG. 3. AS-CDM model. The upper panel is for residual CMB-TT and the bottom panel is for the ratio of MPS with respect to ΛCDM. The AS parameters of the different lines are indicated by the labels.

approaches ΛCDM, making the two practically indistinguishable on large scales. This suppression of matter perturbation growth translates into a weaker gravitational potential, leading to an enhanced CMB at large multipoles, as the potentials are not strong enough to capture the photons. Given the high precision of CMB spectra measurements, this could suggests that the AS-CDM model needs—at least—a larger matter contribution, ω_m to provide a good fit to the data. By doing so, it avoids the reduction of the angular size of the sound horizon θ_s, caused by EDE. An option to achieve this is to increase the h value as the parameter λ decreases. Another approach would be to keep θ_s fixed and then obtain the corresponding h for each λ. In this case, to keep the sound horizon fixed, ω_m will increase as the EDE fraction does.

2. Scalar field dark matter

In the main results, we will focus only on the quadratic and trigonometric potentials because the hyperbolic gives rise to very similar effects to those of the quadratic one [34].

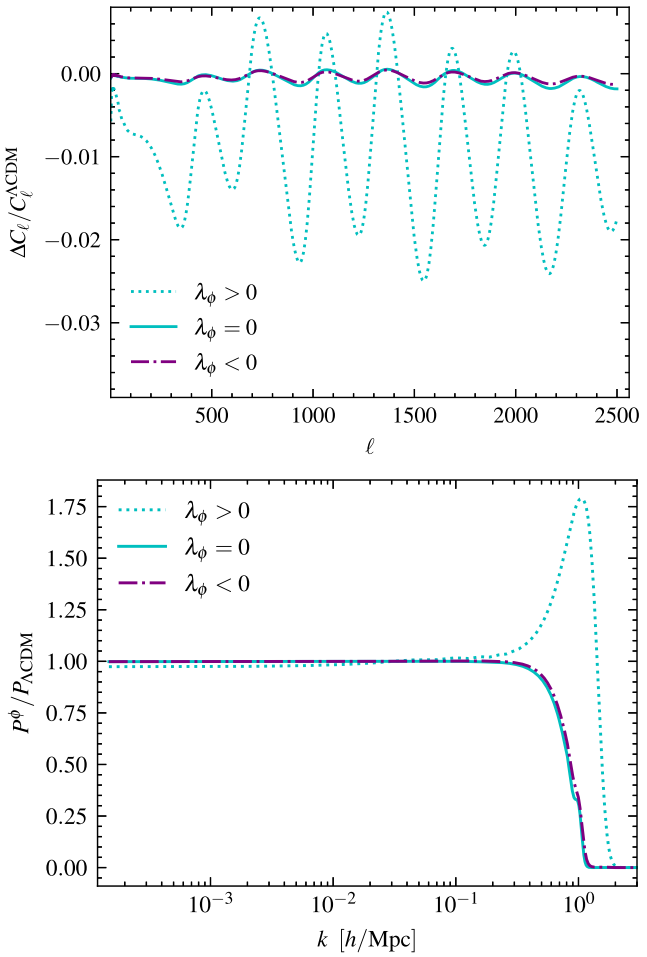

FIG. 4. Λ-SFDM model. Cosmological spectra for the different SFDM potentials, indicated by the labels, all of them for a fixed mass, $m_\phi = 10^{-24}$ eV. The upper panel displays the residual CMB-TT spectra, while the bottom panel shows the MPS ratio relative to ΛCDM.

However, the trigonometric potential exhibits a different behavior, especially in its corresponding MPS, which is significantly different around the cutoff scale, as illustrated in Fig. 4. At the smallest scales, it produces a bump, which is relevant to this work because this behavior is also opposite to the EDE as shown in Fig. 3.

To distinguish the linear effects of the SFDM from that of quintessence, in the plots of Fig. 4, we use a cosmological constant as dark energy ($\Lambda + \mathrm{SFDM}$), and to emphasize the effects for CMB and MPS we chose a smaller mass value rather than the selected for the background plots, and the remaining relevant cosmological parameters were fixed to be the same than in the EDE case; $\omega_b = 0.022$, $\Omega_\phi = 0.264$, $\tau = 0.054$, $A_s = 2.1 \times 10^{-9}$, $n_s = 0.966$, and $h = 0.67$. Note that the CMB-TT remains largely unchanged when considering the hyperbolic and quadratic potentials, but there is a more pronounced deviation with the trigonometric potential. Regarding the MPS ratio, for the same parameter values, the most significant difference with respect to ΛCDM occurs in large wave numbers. However, it is important to note that, overall, the trigonometric potential results in a slightly smaller MPS at large scales.

3. SFDM and quintessence

Considering both scalar fields activated, it is evident from the upper panel of Fig. 5, that the deviations caused by the EDE are partially compensated for by those induced by the scalar field dark matter. For example, the plots illustrate that in this scenario, the deviations caused by EDE in the CMB-TT spectrum are partially counteracted by those generated by SFDM, resulting in a more moderate overall deviation. For instance the angular sound horizon for the considered cosmological parameters is $100\theta_s = 1.041$, for the cosmological standard model, whereas in the AS(ψ)-SFDM(ϕ) model it changes to $100\theta_s = 1.044$ for $\Lambda + \mathrm{SFDM}$, $100\theta_s = 1.033$ for $\mathrm{AS} + \mathrm{CDM}$ and $100\theta_s = 1.039$ when both scalar fields are present.[2] However, the bottom panel of Fig. 5 displays the ratio between the MPS of the scalar fields and the corresponding to ΛCDM. When considering the trigonometric potential for the description of dark matter, the combined effect prevents the suppression of power caused by the EDE, but its characteristic pattern of acoustic oscillations is still present, while simultaneously reducing the size of the bump generated by the nonlinearities of the trigonometric potential.

It is worth recalling that even in the nondirect dark-coupling case, the gravitational influence of both scalar fields is capable to modify the cosmological observables. This is in agreement with the evolution at the background and linear levels of the scalar fields. In particular, the linear contrast density will be discussed in the following section.

IV. INTERACTING CASE

In this section, we turn to the case where a nonminimal coupling between the scalar fields is introduced, and it is added at the level of the KG equations (2), (5). Our equations can incorporate interacting terms that may arise from alternative formalisms, as elaborated in the Appendix B. However, as an illustrative example we focus on a coupling that is proportional to the temporal derivatives of the scalar fields[3]:

[2]The reported angular scale by the Planck collaboration [90] is $100\theta_s = 1.0411 \pm 0.0003$. Given the resultant values above for each model, we see that CMB observations in general are sensitive to the different scenarios, under the same numbers of the cosmological parameters, and could then be used, in a full Bayesian analysis, to put tighter constraints on these possibilities.

[3]This coupling has the advantage of washing out the possible divergences carried by the ratios in Eqs. (2) and its corresponding terms when angular variables are introduced. Notice that within the code the interaction kernel could be easily modifiable.

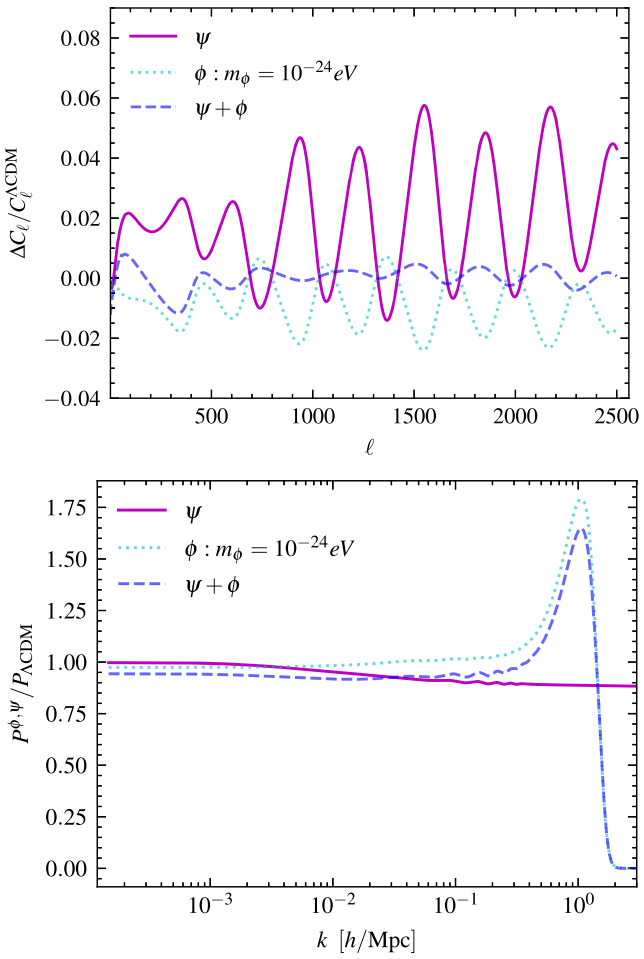

FIG. 5. AS(ψ)-SFDM(ϕ) model. The upper panel shows the residual CMB-TT plot, where $\Delta C_\ell = C_\ell^{\phi,\psi} - C_\ell^{\Lambda CDM}$, while the bottom panel displays the MPS ratio with respect to ΛCDM. In these plots, we are using an SFDM mass of 10^{-24} eV, which differs from the mass used in the background plots, while the quintessence parameters remain the same as before, and all of them have the same $\Omega_m = 0.316$. The dotted line assumes only DM as scalar field (ϕ), the solid line corresponds to DE as quintessence (ψ), and the dashed line represents the scenario where dark matter and dark energy are described as scalar fields without interaction.

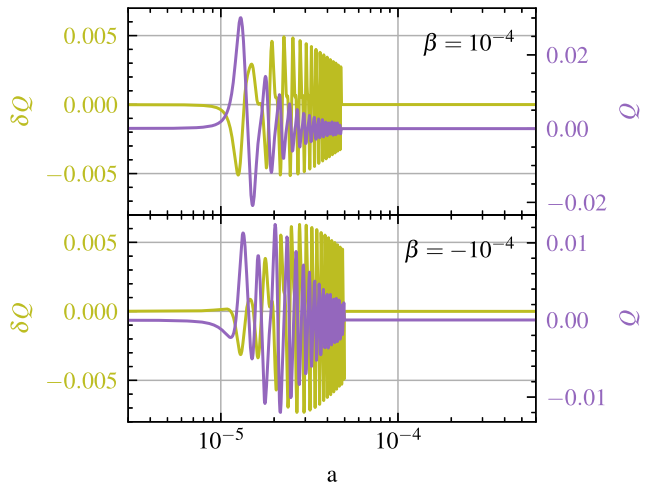

FIG. 6. Interacting $Q - \psi\phi$ model. Evolution of the interacting term according to Eq. (11). The upper panel corresponds to $\beta > 0$, while the bottom panel illustrates the scenario with the opposite sign of β. In both panels, the purple color is for the background level (right vertical axis) and the olive color for linear perturbations (left vertical axis).

$$Q = \beta \dot{\phi} \dot{\psi}, \tag{11}$$

where β is the coupling constant (in units of H_0), the convention adopted in this work is that Q, $\delta Q > 0$ means that SFDM is transferring energy density to the EDE component and, it is important to remark that in this context also the inverse process is possible. A more comprehensive and formal derivation regarding the introduction of the interaction term can be found in the Appendix C.

Just like in the case without a direct interaction, in this section, the EDE is represented by a quintessence scalar field with an AS potential given by Eq. (9), and the SFDM can be described by the potentials presented in Eq. (10) (model $Q - \psi\phi$) and the cosmological parameters are equal to those in previous sections. At the background and linear level, the evolution of the matter densities is sensitive to the value of the constant coupling. For example, for a fixed SFDM mass of 10^{-24} eV, $|\beta|$ values lower than 10^{-4} produce smaller amplitudes or changes less pronounced than those presented in Figs. 6, 7. However, the overall shape remains similar, showing a rescaled pattern. Also, if we consider SFDM masses higher than 10^{-24} eV, the interacting effect is barely noticeable for the same value of β.

For instance, the interaction rate is non-negligible over a range of the scale factor, shown in Fig. 6. This is a consequence in agreement with the proposal that the interacting term is proportional to the kinetic terms of the scalar fields, see Appendix D for more details. Specifically, this has to do with the fact that the SFDM starts oscillating rapidly, with a mean—on average—equal to zero. It is also noticeable that the oscillations of the interaction kernel are changing sign, in both cases of the sign of β, suggesting a bidirectional exchange between SFDM and EDE. A similar change in sign in the interacting kernel, at low redshift, has been found using model-independent techniques [74]. The difference between the upper and lower panels of Fig. 6 is that for $\beta < 0$ the background interaction has a small reduction in amplitude, while at linear order the amplitudes of δQ are enhanced.

In Fig. 7, we can see the effects of the density interchange between SFDM and EDE. It is noticeable that now, where the interaction is relevant, the EDE has an extra contribution ceded by the kinetic term of the SFDM, that is

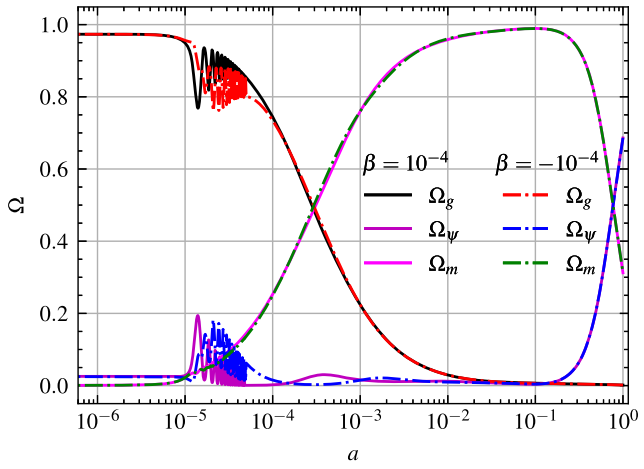

FIG. 7. Evolution of the matter densities when the direct interaction in the dark sector is turned on, with $\beta = \pm 10^{-4}$. Quintessence is described by the AS potential with parameters: $\lambda = 12$, $A = 0.004$, $B = 22.66$, while $\Omega_m = \Omega_b + \Omega_\phi$ with SFDM parameters: $m_\phi = 10^{-24}$ eV, $\lambda_\phi = 10^4$. Solid lines correspond to the $\beta > 0$ case and dashed-dotted lines are for the $\beta < 0$ case. Regardless of the sign of β, the interaction causes EDE to capture the oscillations originally present in the SFDM component.

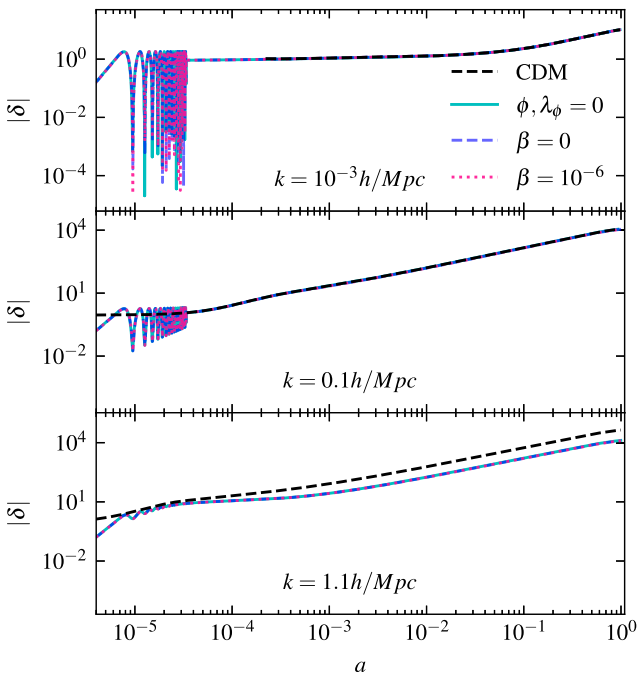

FIG. 8. Evolution of different contrast densities for a quadratic SFDM potential. For the different models the mass of the SFDM is fixed to 10^{-24} eV and the AS parameters are $\lambda = 12$, $A = 0.004$, $B = 22.7$.

reduced for negative values of β. It is also worth noting that the effect we are observing in the radiation component does not indicate that radiation is providing density to EDE. Instead, this is a consequence of the scaling behavior of EDE with respect to radiation. In both cases of Fig. 7, the interaction is diluting while oscillating, and, notably, the global shapes of Ω_ψ exhibit similar patterns. For both signs of β, during the oscillating phase of the interaction, there is a reflected oscillating enhancement of this component (slightly smaller for $\beta < 0$), which then dilutes as the interaction progresses. Subsequently, when the interaction stops, the fields evolve freely and its standard evolution, $\beta = 0$, is recovered.

At the level of linear perturbations, we are able to gain some insights into the effect of the interaction by looking at the evolution of the dark matter fractional density contrasts, $\delta = \delta\rho_{\rm dm}/\rho_{\rm dm}$. In Figs. 8 and 9, we present the evolution of three distinct k modes under different assumptions. For comparison, we include the corresponding evolution of CDM and a case with only dark matter as a scalar field. We will give more emphasis to the trigonometric potential, but a detailed analysis on the quadratic potential can be found in [89].

The mode $k = 10^{-3} h/\text{Mpc}$ oscillates very rapidly until the scale factor reaches a value $a \sim 10^{-5}$, long before it enters the horizon. However, when it crosses the horizon, it grows as CDM, although its strength is slightly lower. At this scale, there is no significant difference when both scalar fields are present, even for the interaction parameter $\beta = 10^{-6}$. However, this could change for different values of the interaction parameter β. From the evolution of the intermediate wave number $k = 0.1\ h/\text{Mpc}$, we notice that it grows very similarly in the SFDM case as in the ΛCDM case, except for earlier times when the density contrast of the SFDM initially experiences suppressed growth. However, it follows the same scaling with a period of rapid oscillations, and eventually scales like the CDM case at late times. The initial suppression is more pronounced for the trigonometric potential than for the quadratic potential. During this period, the interaction term exhibits some differences in growth. Finally, the scale at the wave number $k = 1.1\ h/\text{Mpc}$ enters the horizon before the matter-radiation equality, and it is beyond the characteristic Jeans scale. From the evolution of this and the wave numbers beyond the characteristic cut-off, as shown in Fig. 8, we can see that for the quadratic potential, the evolution of dark matter (DM) is lower than that of cold dark matter (CDM). Consequently, we observe a suppression of power at these scales. However, for the trigonometric potential, the evolution of the density contrast DM in Fig. 9 is not below that of the corresponding CDM; instead, it is slightly larger, resulting in the characteristic bump in the MPS for this potential.

Figure 10 shows the changes in the CMB-TT and matter power spectra for different values of the interaction parameter and considering the trigonometric potential to describe the SFDM component. Concerning the matter power spectra, we observe that when the interaction is

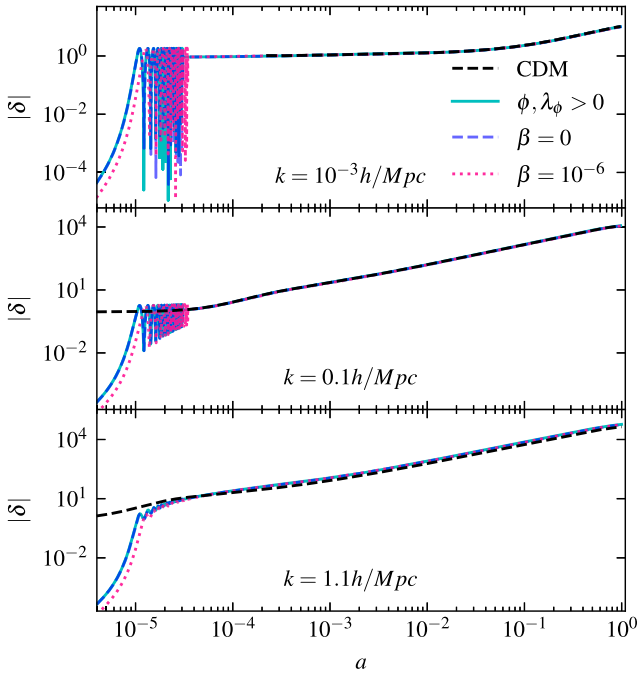

FIG. 9. Evolution of different fractional density contrasts. For the different models the mass of the SFDM is fixed to 10^{-24} eV with a trigonometric potential, $\lambda_\phi = 10^4$. The AS parameters are $\lambda = 12$, $A = 0.004$, $B = 22.7$. The evolution with a negative β value has slightly pronounced and prolonged effects than the $\beta > 0$ scenario.

considered and activated with different values of β, the overall shape of the total spectra closely mimics that of the SFDM. Nevertheless, it also reflects the oscillations of the MPS associated with EDE at intermediate-small scales.

The part of the spectra that corresponds to the early universe (large k modes) reflects that for $\beta \neq 0$ the nonlinearity's associated to the trigonometric potential are not erased by the interaction, instead, they are enhanced regardless of the sign of the interacting parameter. However, the difference is that $\beta > 0$ transfers more of its kinetic term to EDE than in the case $\beta < 0$, so that the spectra of positive β are slightly smaller than the opposite. At intermediate-small scales, where the EDE starts to suppress the spectra, this suppression does not persist to larger k modes as it does in the case of EDE alone. Instead, this suppression is counteracted by the enhancement caused by SFDM.

Finally, on intermediate-large and large scales ($k \lesssim 0.03[h/\mathrm{Mpc}]$), Fig. 10 shows that $\beta < 0$ results in a suppression of power. This might seem counterintuitive, but it is a consequence that these scales bring the horizon around the time when the kinetic term of the EDE field is recovering ($a \gtrsim 1.7 \times 10^{-3}$) and, indeed, its density is slightly greater than that corresponding to the $\beta = 0$ case. By the same epochs, the $\beta > 0$ case experiences an opposite behavior, resulting now in a decrease in EDE at these wave numbers. This makes these transients reflect at the point where the spectra cross.

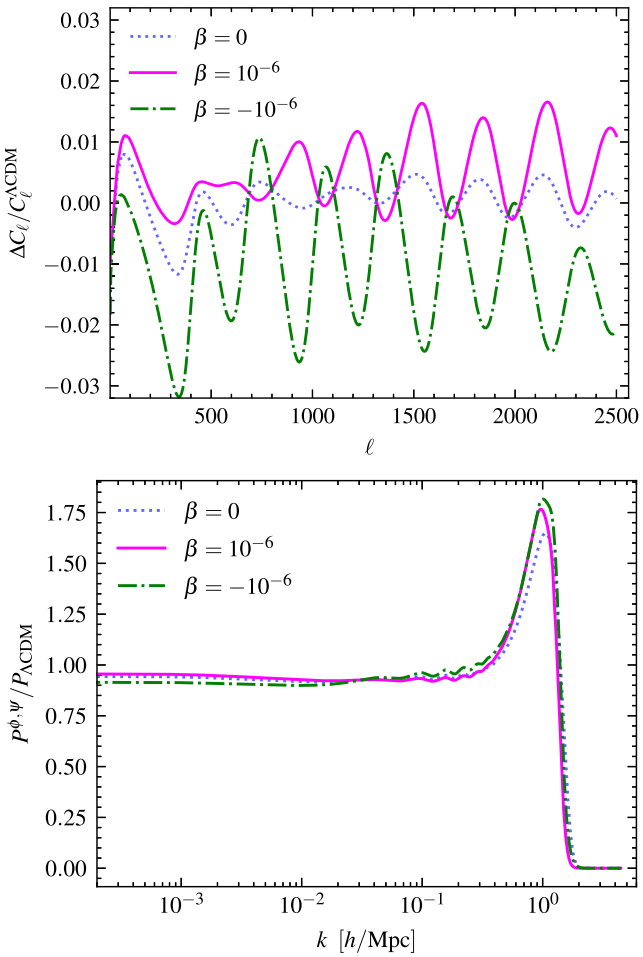

FIG. 10. Upper panel shows the CMB-TT spectra and the bottom exhibits the MPS, both described by the same cosmological and scalar field parameters. The interaction between the scalar fields is considered for different values of β as indicated by the labels. The values of the scalar fields parameters are the same as in Fig. 9.

In relation to the impact on the CMB-TT power spectra, as illustrated in the upper panel of Fig. 10, it is important to remark that the net effect in the residual plots for the chosen parameters is about 3%, compared with the ΛCDM model, however it is important to remark that these deviations could be different if the cosmological parameters were fixed using other basis. Notably, these deviations are more pronounced in the case of $\beta < 0$, where the same $|\beta|$ leads to enhanced perturbations in the considered model of interaction, however the smaller deviations are for the case of nondirect coupling ($\beta = 0$). In alignment with the shape of the MPS, it is observed that the TT spectra now exhibit opposite peaks, suggesting that the corresponding densities lead, on one side, to potential wells with contrary behavior, as expected, while on the other hand they also cause opposite impact on the angular sound horizon. Consequently, the deviations in the CMB-TT spectra naturally differ.

V. CONCLUSIONS

In this work we considered the possibility that both, simultaneously, the dark matter and dark energy can be described by scalar fields each with an associated potential that is able to reproduce the desired behavior, and, on the top of that, incorporating an interaction kernel between them that is consistent with the total conservation equations. This consideration leaves a footprint in the cosmological observables as shown in Figs. 5 and 10, where the MPS and CMB power spectra are plotted for different cases: only one scalar field, two scalar fields coupled only by gravity, and an example of a nonminimal coupling [Eq. (11)] controlled by an interacting kernel Q.

At the background level, when considering both scalar fields, the evolution of their associated matter densities is not altered by the gravitational presence of the other scalar field. However, when a direct interaction is activated, they exchange density; specifically for the chosen interaction, this exchange occurs through an interchange of kinetic energy, whose direction along the scale factor does not always correspond to the sign of β. For example, for a fixed value of β, SFDM does not always yield/gain a part of its density. Instead, during certain periods of time, it receives/losses a contribution coming from EDE. When considering two values of β with the same absolute value but with a change in sign, we observe similar behaviors with a slight decreasing amplitude of the effects carried by $\beta < 0$.

The fluctuations in the background and linear densities caused by each one of the scalar fields imprint characteristic patterns in the cosmological spectra, which can be partially compensated by the direct or nondirect interaction between them. For example, the choice of the SFDM potential results in an MPS with a dramatic suppression of power at large k-modes if the considered potential is quadratic or hyperbolic. In contrast, it exhibits a bump if the potential is trigonometric.

In this respect, we found that the presence of an EDE scalar field component, described by the AS potential, can partially counteract these effects, as shown in Figs. 5 and 10. However, at these scales, the effects of SFDM are predominant over those from EDE, and thus the mechanism is not enough to entirely prevent the dramatic suppression of the MPS or eliminate the bump, whether there is a direct or nondirect interaction between the fields. Moreover, we find that the most significant attenuation occurs when the coupling is only gravitational, in contrast to the interaction described by the term (11), which, for example, increases the nonlinearities.

At large and intermediate scales the main characteristics of the SFDM are preserved, but now, even the global shape is unchanged, we expect small deviations with respect to ΛCDM depending the value of β carried out by the over/underdensities created by the exchange of the kinetic term between the fields, as already explained in the text, this behavior is opposite for the same magnitude of the interaction but with different sign.

Finally, concerning the MPS, it is also important to mention that now the suppression of power associated to the presence of a pure EDE field is avoided, this is relevant because it is common to compensate for this suppression by adding extra ω_c. The addition of this component is required to not alter other observables, for example, without it the potential wells and the angular sound horizon decreases, causing an enhanced CMB-TT spectrum. In that sense, a very important result is that in this scenario, may be no needs to add additional ω_c to have CMB-TT power spectra whose deviations could be in agreement with the data, for example, for the chosen parameters, we obtain deviations up to 3% that can be lowered by different values of β.

Performing a Bayesian analysis to constrain the parameters of the interacting model along with those from the cosmological standard model is one of the future perspectives of this research. Up to this point, this study offers valuable insights into the intricate dynamics of the cosmological dark sector described by different scalar fields, and also provides a general formalism to implement different couplings between them, which can help to overcome some of the disadvantages associated with the models of a single scalar field. Furthermore, the specific interaction discussed has been incorporated into a publicly available modification of a CLASS code, enabling the easy inclusion of different couplings to expand the scope of the analysis concerning interacting scalar fields.

ACKNOWLEDGMENTS

G.G-A. acknowledges CONAHCYT postdoctoral fellowship and the support of the ICF-UNAM. L. A.U-L. acknowledges partial support from the Programa para el Desarrollo Profesional Docente; Dirección de Apoyo a la Investigación y al Posgrado, Universidad de Guanajuato; CONACyT México under Grants No. 286897, No. 297771, No. 304001; and the Instituto Avanzado de Cosmología Collaboration. J. A. V. acknowledges the support provided by FOSEC SEP-CONACYT Investigación Básica A1-S-21925, UNAM-DGAPA-PAPIIT IN117723 and FORDECYT-PRONACES-CONACYT/304001/2019.

APPENDIX A: ANALYSIS OF THE AS QUINTESSENCE POTENTIAL

The standard parametrization of the AS potential is a bit confusing, so for a better understanding of its intrinsic properties, we will consider the following changes. First, we make a change in the scalar field: $\psi - B \to \psi$, which leaves the KG equation of motion unchanged. Secondly, we write the AS potential as

$$V(\psi) = \left(\mu^2 f^2 + \frac{1}{2}\mu^2\psi^2\right) e^{-\lambda\kappa\psi}, \tag{A1}$$

where the new parameters μ and f have the dimensions of energy, and λ is now explicitly dimensionless in the exponential term. Note that the polynomial part of the potential (A1) is parametrized as usual for these kinds of potentials.

The calculation of the critical points ψ_c of the potential (A1) is quite straightforward, and from condition $V'(\psi_c) = 0$ we obtain

$$\lambda\kappa\psi_c = 1 \pm \sqrt{1 - 2\lambda^2\kappa^2 f^2}. \tag{A2}$$

Then, the second derivative at the critical points is

$$V''(\psi_c) = \mp\sqrt{1 - 2\lambda^2\kappa^2 f^2}\,\mu^2 e^{-\lambda\kappa\psi_c}, \tag{A3}$$

which means that the critical point ψ_c corresponding to the minus (plus) sign in Eq. (A2) is a minimum (maximum).

Another important result is the value of the potential (A1) at the minimum, as this value would be the effective cosmological constant that the model provides once the field evolves towards its critical value. The result is

$$\Lambda_{\text{eff}} = V(\psi_c) = \frac{\mu^2}{\lambda\kappa}\psi_c e^{-\lambda\kappa\psi_c}. \tag{A4}$$

Being a minimum, the scalar field oscillates rapidly as it settles down into this critical point.

We can see the advantages of the new parametrization in Eq. (A1): the parameter μ plays the role of a bare mass of the scalar field ψ,[4] while f is a new energy scale that determines the position of the critical points of the potential. With respect to the parameter f, we can consider two extreme cases. The first is $f = 0$, which results in the potential

$$V(\psi) = \frac{1}{2}\mu^2\psi^2 e^{-\lambda\kappa\psi}, \tag{A5}$$

with critical points at the values $\lambda\kappa\psi_c = 1 \pm 1$. However, in this case, there is no effective cosmological constant at late times, as we can see from Eq. (A4) that $\Lambda_{\text{eff}} = 0$.

Another case of interest is $2\lambda\kappa f = 1$, for which there is only one critical value of the scalar field: $\lambda\kappa\psi_c = 1$, which is also an inflection point. The field potential now reads

$$V(\psi) = \left(\mu^2 f^2 + \frac{1}{2}\mu^2\psi^2\right)e^{-\lambda\kappa\psi}, \tag{A6}$$

which means that the field continues rolling down the potential, but this time without oscillations at all.

[4]Recall that the effective mass of the field is given by $m^2_{\text{eff}} = V''(\psi_c)$, and then $\mu^2_{\text{eff}} \propto \mu^2$.

APPENDIX B: ALTERNATIVE FORMALISM FOR A COUPLING

$$\ddot{\psi} + 3H\dot{\psi} + \partial_\psi V(\psi) = -\Gamma_\psi\dot{\psi}. \tag{B1a}$$

Such a friction term is standard in models of inflation to study the decay of the inflation field into other particles, where Γ represents the decay rate of the scalar field calculated from a given coupling. If we multiply Eq. (B1a) by $\dot{\psi}$ on both sides, we can rewrite it in terms of energy density and pressure, as[5]

$$\dot{\rho}_\psi + 3H(\rho_\psi + p_\psi) = Q_\psi = -\Gamma_\psi\dot{\psi}^2. \tag{B1b}$$

If we repeat the exercise for the DM field, we arrive to the counterpart of Eq. (B1) for the field ϕ,

$$\ddot{\phi} + 3H\dot{\phi} + \partial_\phi V(\phi) = \Gamma_\phi\dot{\phi}. \tag{B2a}$$

which in turn leads us to the counterpart of Eq. (B1b),

$$\dot{\rho}_\phi + 3H(\rho_\phi + p_\phi) = Q_\phi = \Gamma_\phi\dot{\phi}^2. \tag{B2b}$$

As mentioned above, the conservation of the total density, for the coupled DM-DE fields in terms of $Q_\psi = -Q_\phi$, then requires $\Gamma_\phi\dot{\phi}^2 = \Gamma_\psi\dot{\psi}^2$. Motivated by arguments of symmetry between the interacting fields, we propose here that the coupling between the fields is of the form

$$Q_\phi = -Q_\psi = \Gamma\dot{\phi}^2\dot{\psi}^2, \tag{B3a}$$

where Γ would be a constant with the appropriate units. Another form of Eq. (B3) can be found if we write the kinetic terms using the definitions of the density and pressure for each field, and then

$$\Gamma\dot{\phi}^2\dot{\psi}^2 = \Gamma(\rho_\phi + p_\phi)(\rho_\psi + p_\psi). \tag{B3b}$$

Equation (B3b) has an additional advantage, in addition to its symmetrical form, which is that interactions between two fields should involve both energy densities, so a quadratic form could be considered a more natural choice [93]. For example, the decay rate of the field ψ would be effectively given by $\Gamma_\psi = \Gamma\dot{\phi}^2$, and likewise for the decay rate of the

[5]A quick comparison with the standard formalism of coupled perfect fluids in cosmology suggests that the term on the right-hand side of Eq. (B1b) has the expected form in isentropic creation/annihilation of particles, that is, the entropy per particle remains constant. Furthermore, we could identify Γ_ψ as the rate of change of the number of particles in a comoving volume a^3. See [91,92] for a detailed discussion of the thermodynamics of two interacting cosmological fluids.

field ϕ: $\Gamma_\phi = \Gamma\dot{\psi}^2$. Furthermore, the sum of density and pressure in Eq. (B3b) also hints at the possibility that the coupling functions Q_ϕ, Q_ψ could be seen as extra friction terms in the equations of motion (B1b) and (B2b).

APPENDIX C: THE FLUID APPROXIMATION FOR THE COUPLED DARK SECTOR

$$\nabla_\nu T^{\mu\nu}_\phi = \phi^{,\mu}[\Box\phi - \partial_\phi V(\phi)] = Q^\mu_\phi, \tag{C1}$$

$$\nabla_\nu T^{\mu\nu}_\psi = \psi^{,\mu}[\Box\psi - \partial_\psi V(\psi)] = Q^\mu_\psi, \tag{C2}$$

where $\Box$ is the Laplace-Beltrami operator, and the terms Q^μ are called the (covariant) energy-momentum transfer rates. We must impose the condition $Q^\mu_\phi = -Q^\mu_\psi$, so that the conservation of the joint energy is achieved by the two components in the form $\nabla_\nu(T^{\mu\nu}_\phi + T^{\mu\nu}_\psi) = 0$.

Generally, the coupling term for each field can be written as $Q^\mu = Qu^\mu + F^\mu$, where u^μ is the total four-velocity [94]. We refer to Q as the parallel component, since $Q^\mu u_\mu = -Q$, and represents the transfer of energy, while F^μ is the perpendicular component that satisfies the condition $F^\mu u_\mu = 0$, and represents the transfer of momentum. For simplicity, in this study we shall assume that only energy is exchanged between the dark components, i.e., $F^\mu = 0$.

According to [95,96], the four-velocity of the scalar fields in the dark sector can be written as

$$u^\mu_\psi = \frac{\psi^{,\mu}}{\sqrt{-\psi_{,\mu}\psi^{,\mu}}}, \qquad u^\mu_\phi = \frac{\phi^{,\mu}}{\sqrt{-\phi_{,\mu}\phi^{,\mu}}}, \tag{C3}$$

so that both of them comply with the normalization condition $u_\mu u^\mu = -1$. With these definitions, the KG equations of motion for the fields read

$$\Box\phi - \partial_\phi V(\phi) = -\frac{\phi_{,\mu}Q^\mu_\phi}{\phi_{,\mu}\phi^{,\mu}}, \tag{C4a}$$

$$\Box\psi - \partial_\psi V(\psi) = -\frac{\psi_{,\mu}Q^\mu_\psi}{\psi_{,\mu}\psi^{,\mu}}. \tag{C4b}$$

It is then possible to recover the equations of motion (B1b) and (B2b) if we choose the following coupling terms for each field.

$$Q^\mu_\phi = \Gamma_\phi(\phi_{,\mu}\phi^{,\mu})u^\mu_\phi, \qquad Q^\mu_\psi = \Gamma_\psi(\psi_{,\mu}\psi^{,\mu})u^\mu_\psi. \tag{C5}$$

Notice that Eqs. (C5) also gives more support to our choice of the phenomenological coupling in Eqs. (B1b) and (B2b): the coupling is proportional in each case to an invariant quantity, which is the norm of the covariant derivative of the fields. More to the point, if we see the fields as a joint dark sector, Eqs. (B3) can be further written as

$$Q^\mu_\phi = \Gamma(\phi_{,\mu}\phi^{,\mu})(\psi_{,\mu}\psi^{,\mu})u^\mu_\phi, \tag{C6a}$$

$$Q^\mu_\psi = -\Gamma(\phi_{,\mu}\phi^{,\mu})(\psi_{,\mu}\psi^{,\mu})u^\mu_\psi. \tag{C6b}$$

Thus, the covariant transfer rates (C6) are again symmetrical with respect to the fields ϕ, ψ.

APPENDIX D: UNIDIRECTIONAL ENERGY TRANSFER BETWEEN SCALAR FIELDS

The energy coupling $Q = \beta\dot{\psi}\dot{\phi}$ is symmetric under the fields ψ and ϕ, which means that the transfer of energy proceeds as long as the fields roll down their potentials with a non-negligible kinetic energy. However, the transfer of energy can be interrupted for one of the fields if there are rapid oscillations in their evolution, as we shall show with a simple example.

The KG equations (2) are written explicitly as,

$$\ddot{\psi} + 3H\dot{\psi} + \partial_\psi V(\psi) = -\beta\dot{\phi}, \tag{D1a}$$

$$\ddot{\phi} + 3H\dot{\phi} + \partial_\phi V(\phi) = \beta\dot{\psi}. \tag{D1b}$$

We assume the evolution of the fields at late times, so that the SFDM field rapidly oscillates around the minimum of its potential. Under this circumstance, we can see that on average $\langle\beta\dot{\phi}\rangle \simeq 0$, which means that there is no energy extraction from the EDE field and then it effectively evolves as an uncoupled field. In contrast, for the SFDM field we find that $\beta\dot{\psi} \neq 0$, as long as $\dot{\psi} \neq 0$ for the EDE field.

More precisely, the new KG equations are

$$\ddot{\psi} + 3H\dot{\psi} + \partial_\psi V(\psi) = 0, \tag{D2a}$$

$$\ddot{\phi} + 3H\dot{\phi} + \partial_\phi V(\phi) = \beta\dot{\psi}. \tag{D2b}$$

Interestingly enough, we have the situation in which one of the fields evolves freely, while at the same time the other field has its evolution modified by a nonhomogeneous term in the KG equation for the field ϕ.

Notice that this is consistent with the equations of motion in terms of the energy densities of the fields. If we recall that

$$\dot{\rho}_\psi = -3H(\rho_\psi + p_\psi) - \beta\dot{\phi}\dot{\psi}, \tag{D3a}$$

$$\dot{\rho}_\psi = -3H(\rho_\phi + p_\phi) + \beta\dot{\phi}\dot{\psi}\,. \tag{D3b}$$

Taking into account the rapid oscillations of the field ϕ, we can see that $\langle\beta\dot{\phi}\dot{\psi}\rangle \simeq \beta\dot{\psi}\langle\dot{\phi}\rangle \simeq 0$, and then at the level of the energy densities, the fields on average do not exchange energy.

[1] S. Perlmutter *et al.* (Supernova Cosmology Project Collaboration), Astrophys. J. **517**, 565 (1999).
[2] P. Astier *et al.* (SNLS Collaboration), Astron. Astrophys. **447**, 31 (2006).
[3] T. Bernal, L. M. Fernández-Hernández, T. Matos, and M. A. Rodríguez-Meza, Mon. Not. R. Astron. Soc. **475**, 1447 (2018).
[4] P. J. E. Peebles and B. Ratra, Rev. Mod. Phys. **75**, 559 (2003).
[5] T. Padmanabhan, Phys. Rep. **380**, 235 (2003).
[6] E. Abdalla *et al.*, J. High Energy Astrophys. **34**, 49 (2022).
[7] D. H. Weinberg, J. S. Bullock, F. Governato, R. Kuzio de Naray, and A. H. G. Peter, Proc. Natl. Acad. Sci. U.S.A. **112**, 12249 (2015).
[8] P. Bull *et al.*, Phys. Dark Universe **12**, 56 (2016).
[9] J.-w. Lee and I.-g. Koh, Phys. Rev. D **53**, 2236 (1996).
[10] T. Matos and F. S. Guzman, Classical Quantum Gravity **17**, L9 (2000).
[11] T. Matos, F. S. Guzman, and L. A. Urena-Lopez, Classical Quantum Gravity **17**, 1707 (2000).
[12] W. Hu, R. Barkana, and A. Gruzinov, Phys. Rev. Lett. **85**, 1158 (2000).
[13] P. J. E. Peebles and B. Ratra, Astrophys. J. Lett. **325**, L17 (1988).
[14] R. R. Caldwell, R. Dave, and P. J. Steinhardt, Phys. Rev. Lett. **80**, 1582 (1998).
[15] P. J. Steinhardt, Phil. Trans. R. Soc. A **361**, 2497 (2003).
[16] E. J. Copeland, A. R. Liddle, and D. Wands, Phys. Rev. D **57**, 4686 (1998).
[17] A. H. Guth, Phys. Rev. D **23**, 347 (1981).
[18] A. D. Linde, Phys. Lett. **108B**, 389 (1982).
[19] A. Albrecht and P. J. Steinhardt, Phys. Rev. Lett. **48**, 1220 (1982).
[20] J. S. Alcaniz and F. C. Carvalho, Europhys. Lett. **79**, 39001 (2007).
[21] S.-J. Sin, Phys. Rev. D **50**, 3650 (1994).
[22] J.-w. Lee and I.-g. Koh, Phys. Rev. D **53**, 2236 (1996).
[23] F. Guzmán, T. Matos, and H. Villegas, Astron. Nachr. **320**, 97 (1999).
[24] T. Matos, A. Vazquez-Gonzalez, and J. Magana, Mon. Not. R. Astron. Soc. **393**, 1359 (2009).
[25] A. Suárez, V. H. Robles, and T. Matos, Astrophys. Space Sci. Proc. **38**, 107 (2014).
[26] M. Y. Khlopov, B. A. Malomed, I. B. Zeldovich, and Y. B. Zeldovich, Mon. Not. R. Astron. Soc. **215**, 575 (1985).
[27] L. E. Padilla, J. A. Vázquez, T. Matos, and G. Germán, J. Cosmol. Astropart. Phys. 05 (2019) 056.
[28] B. Li, T. Rindler-Daller, and P. R. Shapiro, Phys. Rev. D **89**, 083536 (2014).
[29] A. Suárez and P.-H. Chavanis, Phys. Rev. D **92**, 023510 (2015).
[30] G. G. Ross, G. German, and J. A. Vazquez, J. High Energy Phys. 05 (2016) 010.
[31] F. X. L. Cedeño, A. X. González-Morales, and L. A. Ureña López, Phys. Rev. D **96**, 061301 (2017).
[32] T. Matos, J.-R. Luévano, I. Quiros, L. A. Ureña-López, and J. A. Vázquez, Phys. Rev. D **80** (2009).
[33] L. A. Ureña López, J. Cosmol. Astropart. Phys. 06 (2019) 009.
[34] F. X. Linares Cedeño and L. A. Ureña lópez, Astron. Nachr. **342**, 404 (2021).
[35] L. O. Téllez-Tovar, T. Matos, and J. A. Vázquez, Phys. Rev. D **106**, 123501 (2022).
[36] S. Tsujikawa, Classical Quantum Gravity **30**, 214003 (2013).
[37] E. V. Linder, Gen. Relativ. Gravit. **40**, 329 (2008).
[38] R. R. Caldwell and E. V. Linder, Phys. Rev. Lett. **95**, 141301 (2005).
[39] G. Pantazis, S. Nesseris, and L. Perivolaropoulos, Phys. Rev. D **93**, 103503 (2016).
[40] A. I. Lonappan, S. Kumar, Ruchika, B. R. Dinda, and A. A. Sen, Phys. Rev. D **97**, 043524 (2018).
[41] N. Roy, A. X. Gonzalez-Morales, and L. A. Ureña López, Phys. Rev. D **98**, 063530 (2018).
[42] J. A. Vázquez, D. Tamayo, A. A. Sen, and I. Quiros, Phys. Rev. D **103**, 043506 (2021).
[43] A. Banerjee, H. Cai, L. Heisenberg, E. O. Colgáin, M. M. Sheikh-Jabbari, and T. Yang, Phys. Rev. D **103**, L081305 (2021).
[44] Y.-F. Cai, E. N. Saridakis, M. R. Setare, and J.-Q. Xia, Phys. Rep. **493**, 1 (2010).
[45] K. Bamba, S. Capozziello, S. Nojiri, and S. D. Odintsov, Astrophys. Space Sci. **342**, 155 (2012).
[46] J. A. Vázquez, D. Tamayo, G. Garcia-Arroyo, I. Gómez-Vargas, I. Quiros, and A. A. Sen, Phys. Rev. D **109**, 023511 (2024).
[47] L. P. Chimento, M. I. Forte, R. Lazkoz, and M. G. Richarte, Phys. Rev. D **79**, 043502 (2009).
[48] C. van de Bruck, G. Poulot, and E. M. Teixeira, J. Cosmol. Astropart. Phys. 07 (2023) 019.
[49] L. A. Escamilla and J. A. Vazquez, Eur. Phys. J. C **83**, 251 (2023).
[50] J. Alberto Vazquez, M. Bridges, M. P. Hobson, and A. N. Lasenby, J. Cosmol. Astropart. Phys. 09 (2012) 020.
[51] S. Hee, J. A. Vázquez, W. J. Handley, M. P. Hobson, and A. N. Lasenby, Mon. Not. R. Astron. Soc. **466**, 369 (2017).
[52] G.-B. Zhao *et al.*, Nat. Astron. **1**, 627 (2017).
[53] M. Doran and G. Robbers, J. Cosmol. Astropart. Phys. 06 (2006) 026.
[54] P. Agrawal, F.-Y. Cyr-Racine, D. Pinner, and L. Randall, Phys. Dark Universe **42**, 101347 (2023).
[55] V. Poulin, T. L. Smith, T. Karwal, and M. Kamionkowski, Phys. Rev. Lett. **122**, 221301 (2019).
[56] M. Doran and G. Robbers, J. Cosmol. Astropart. Phys. 06 (2006) 026.
[57] V. Poulin, T. L. Smith, and T. Karwal, Phys. Dark Universe **42**, 101348 (2023).
[58] L. Hui, J. P. Ostriker, S. Tremaine, and E. Witten, Phys. Rev. D **95**, 043541 (2017).
[59] K. K. Rogers, R. Hložek, A. Laguë, M. M. Ivanov, O. H. E. Philcox, G. Cabass, K. Akitsu, and D. J. E. Marsh, J. Cosmol. Astropart. Phys. 06 (2023) 023.
[60] J. Barrow, R. Bean, and J. Magueijo, Mon. Not. R. Astron. Soc. **316**, L41 (2000).
[61] A. Albrecht and C. Skordis, Phys. Rev. Lett. **84**, 2076 (2000).
[62] A. Adil, A. Albrecht, and L. Knox, Phys. Rev. D **107**, 063521 (2023).
[63] J. Magaña and T. Matos, J. Phys. Conf. Ser. **378**, 012012 (2012).
[64] L. A. Ureña López, Front. Astron. Space Sci. **6**, 47 (2019).

[65] P. Mocz *et al.*, Phys. Rev. Lett. **123**, 141301 (2019).
[66] D. Benisty and E. I. Guendelman, Classical Quantum Gravity **36**, 095001 (2019).
[67] K. Bamba, S. D. Odintsov, and P. V. Tretyakov, Eur. Phys. J. C **75**, 344 (2015).
[68] J. A. Vázquez, L. E. Padilla, and T. Matos, Rev. Mex. Fis. E **17**, 73 (2020).
[69] O. Bertolami, P. Carrilho, and J. Páramos, Phys. Rev. D **86**, 103522 (2012).
[70] C. G. Boehmer, N. Tamanini, and M. Wright, Phys. Rev. D **91**, 123002 (2015).
[71] C. G. Boehmer, N. Tamanini, and M. Wright, Phys. Rev. D **91**, 123003 (2015).
[72] W. J. Potter and S. Chongchitnan, J. Cosmol. Astropart. Phys. 09 (2011) 005.
[73] E. Di Valentino, A. Melchiorri, O. Mena, and S. Vagnozzi, Phys. Rev. D **101**, 063502 (2020).
[74] L. A. Escamilla, O. Akarsu, E. Di Valentino, and J. A. Vazquez, J. Cosmol. Astropart. Phys. 11 (2023) 051.
[75] W. Yang, S. Pan, O. Mena, and E. Di Valentino, J. High Energy Astrophys. **40**, 19 (2023).
[76] L. Amendola, Phys. Rev. D **62**, 043511 (2000).
[77] R. Kase and S. Tsujikawa, Phys. Rev. D **101**, 063511 (2020).
[78] P. Pérez, U. Nucamendi, and R. De Arcia, Eur. Phys. J. C **81**, 1063 (2021).
[79] A. A. Costa, L. C. Olivari, and E. Abdalla, Phys. Rev. D **92**, 103501 (2015).
[80] R. An, A. A. Costa, L. Xiao, J. Zhang, and B. Wang, Mon. Not. R. Astron. Soc. **489**, 297 (2019).
[81] L. W. K. Goh, J. Bachs-Esteban, A. Gómez-Valent, V. Pettorino, and J. Rubio, Phys. Rev. D **109**, 023530 (2024).
[82] A. Gómez-Valent, Z. Zheng, L. Amendola, C. Wetterich, and V. Pettorino, Phys. Rev. D **106**, 103522 (2022).
[83] J. Valiviita, E. Majerotto, and R. Maartens, J. Cosmol. Astropart. Phys. 07 (2008) 020.
[84] E. Majerotto, J. Väliviita, and R. Maartens, Mon. Not. R. Astron. Soc. **402**, 2344 (2010).
[85] L. A. Ureña López and A. X. Gonzalez-Morales, J. Cosmol. Astropart. Phys. 07 (2016) 048.
[86] N. Roy, Gen. Relativ. Gravit. **55**, 115 (2023).
[87] C.-P. Ma and E. Bertschinger, Astrophys. J. **455**, 7 (1995).
[88] C. Skordis and A. Albrecht, Phys. Rev. D **66**, 043523 (2002).
[89] R. Hlozek, D. Grin, D. J. E. Marsh, and P. G. Ferreira, Phys. Rev. D **91**, 103512 (2015).
[90] N. Aghanim *et al.* (Planck Collaboration), Astron. Astrophys. **641**, A6 (2020); **652**, C4(E) (2021).
[91] W. Zimdahl, J. Triginer, and D. Pavón, Phys. Rev. D **54**, 6101 (1996).
[92] W. Zimdahl and D. Pavón, Gen. Relativ. Gravit. **33**, 791 (2001).
[93] C. G. Böhmer, G. Caldera-Cabral, N. Chan, R. Lazkoz, and R. Maartens, Phys. Rev. D **81**, 083003 (2010).
[94] J. Väliviita, E. Majerotto, and R. Maartens, J. Cosmol. Astropart. Phys. 07 (2008) 020.
[95] O. F. Piattella, J. C. Fabris, and N. Bilić, Classical Quantum Gravity **31**, 055006 (2014).
[96] V. Faraoni, S. Giardino, A. Giusti, and R. Vanderwee, Eur. Phys. J. C **83**, 24 (2023).